

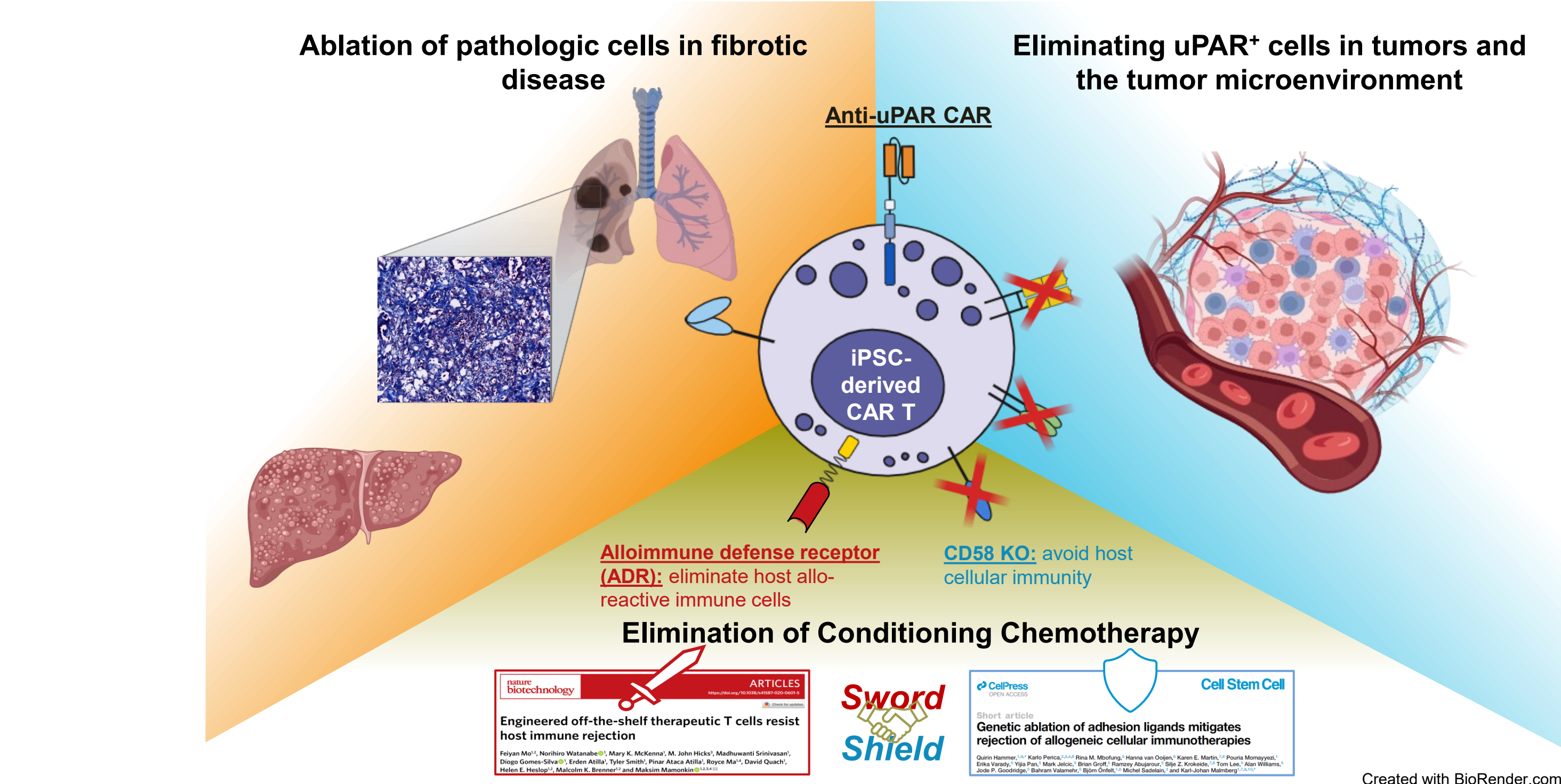
Targeting uPAR with Multiplexed-Engineered iPSC-Derived CAR T Cells to Reverse Age- and Insult-Related Fibrotic Disease

Sean P. Sherman¹, Olena A. Kolesnichenko¹, Thomas Dailey¹, Somayeh Pouyanfar¹, Mochtar Pribadi¹, Masanao Tsuda¹, Hui-Yi Chu¹, Alex J. Garcia¹, Martin P. Hosking¹, Tom Lee¹, Jode Goodridge¹, Eigen Peralta¹, Bahram Valamehr¹

¹Fate Therapeutics, Inc., San Diego, CA, USA

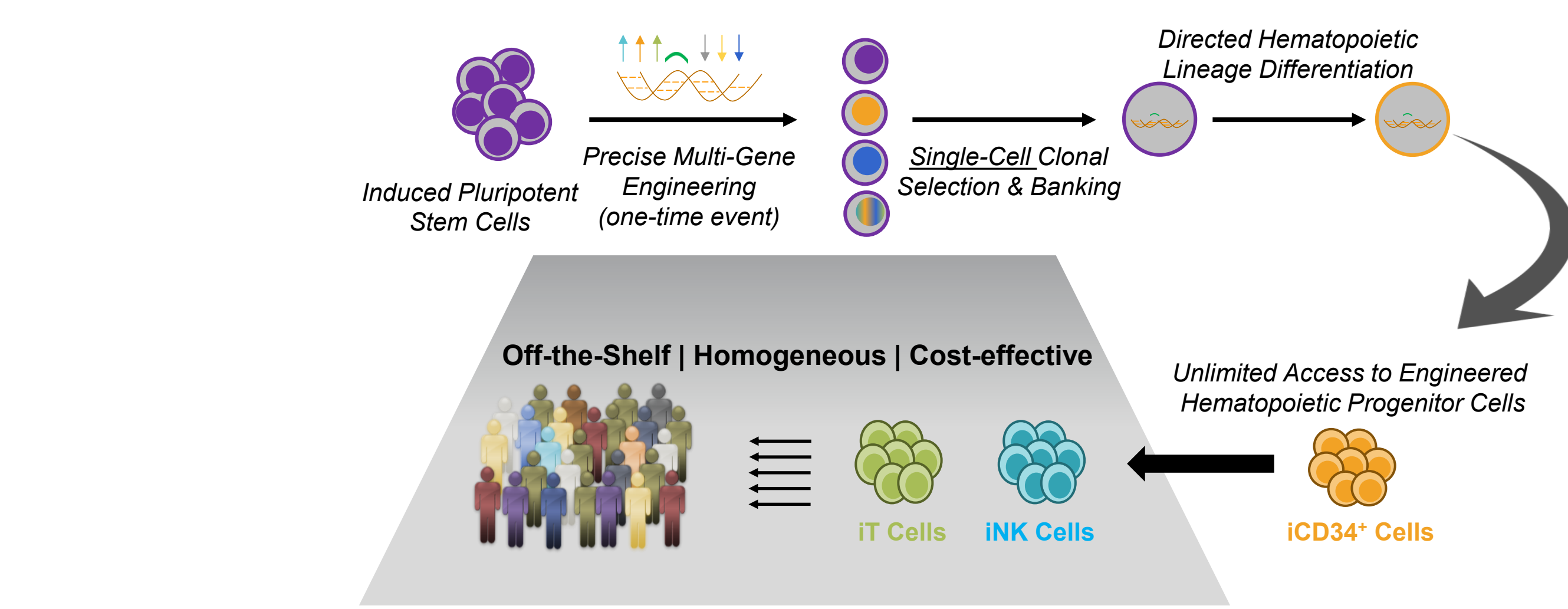
Introduction

Urokinase plasminogen activator receptor (uPAR) is a component of the plasminogen system, contributing to diverse biological processes including fibrinolysis, cell adhesion, and cell migration. Increased uPAR expression has been implicated in cancer and inflammatory disease. Recent work has demonstrated that treatment with anti-uPAR CAR T cells can eliminate fibrosis and restore liver function in models of metabolic dysfunction-associated steatohepatitis (MASH). Here, we present the development of novel anti-uPAR CAR constructs, characterization of uPAR as a target in MASH, radiation induced pulmonary fibrosis (RIPF), and cancer, and development of iPSC-derived CAR T cells for treatment of multiple disease indications.



In addition to developing CAR T cells targeting human uPAR, we have developed a new mouse model for targeting uPAR in RIPF. In humans, RIPF is a common side effect of radiation therapy with minimal treatment options. In preclinical studies, after a single dose of radiation to the left lung, we observed significant fibrosis in the irradiated tissue within two weeks. As in models of liver fibrosis, uPAR expression was upregulated in the fibrotic region following irradiation, evidence that targeting uPAR⁺ cells with CAR T-cell therapy will be widely applicable to a range of fibrotic diseases with few current therapeutic options. Moreover, targeting either fibrotic diseases such as MASH and RIPF or cancers with iPSC-derived CAR T cells will avoid drawbacks of traditional CAR T-cell therapy including manufacturing challenges overcome by our off-the-shelf approach and the need for conditioning chemotherapy mitigated by our sword and shield technology.

Multiplexed-engineering iPSC platform overcomes multiple challenges associated with existing approaches to cellular therapy



Summary & Conclusions

- The urokinase plasminogen activator receptor (uPAR) plays a role in diverse biological processes and its expression is increased in multiple pathologic contexts including inflammation, fibrosis, and cancer.
- Recent work has demonstrated the ability of uPAR CAR T cells to ameliorate fibrosis and restore liver function in mouse models of MASH. Here, we describe a similar pattern of uPAR staining in human MASH patients, presenting an opportunity for a CAR T cell therapy to target MASH.
- Similar to MASH, radiation induced pulmonary fibrosis (RIPF) is a common disease with no currently available treatments other than management of symptoms. Here, we describe a mouse model of RIPF characterized by rapid development of fibrosis and upregulation of uPAR expression, confirming uPAR as a therapeutic target across multiple fibrotic diseases.
- Because domain 1 of uPAR is frequently cleaved, we developed a series of target cell lines to classify candidate binders by binding location. By correlating MASH patient IHC staining for uPAR with in vitro target cell lines we also characterize candidate binders by their ability to specifically target pathologic levels of uPAR expression.
- uPAR is highly expressed on multiple tumor model cell lines, and human primary uPAR CAR T cells show effective control of tumor growth in vitro and in vivo.
- iPSC-derived uPAR CAR T cells exhibit unique and potent elimination of uPAR expressing targets and enable the potential for an off-the-shelf CAR T cell therapy for the treatment of age- and insult-related fibrotic disease.

Results

uPAR is expressed in fibrotic cells in MASH patient samples

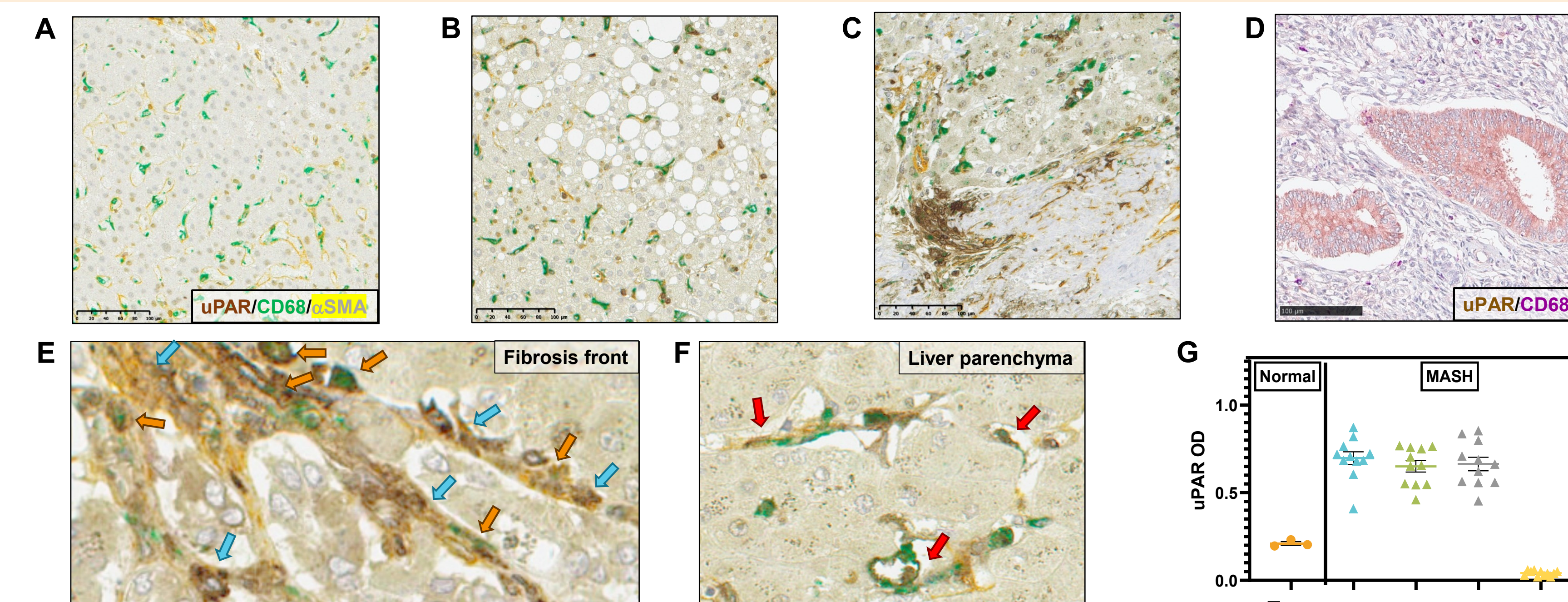


Figure 1. Characterization of uPAR as a target in fibrotic disease. uPAR is not observed in normal patient liver samples (A) but is present in patients with moderate (B, Stage 2) to severe (C, Stage 4) MASH. uPAR expression was low in other normal tissue samples, including uterine tissue (D). In fibrotic liver (E), uPAR is highly localized with CD68⁺ macrophages (orange) and α SMA⁺ (activated) hepatic stellate cells (blue). uPAR also co-localizes with macrophages and activated hepatic stellate cells in fibrosis-adjacent parenchyma (F) of MASH patients. Quantification of uPAR IHC (G) demonstrates low levels of uPAR in normal tissue and hepatocytes of MASH patients, with high levels of uPAR in the macrophages, hepatic stellate cells, and other inflammatory cell types in MASH patient livers.

A single dose of focal radiation to the left lung induces fibrosis and uPAR expression within 2 weeks

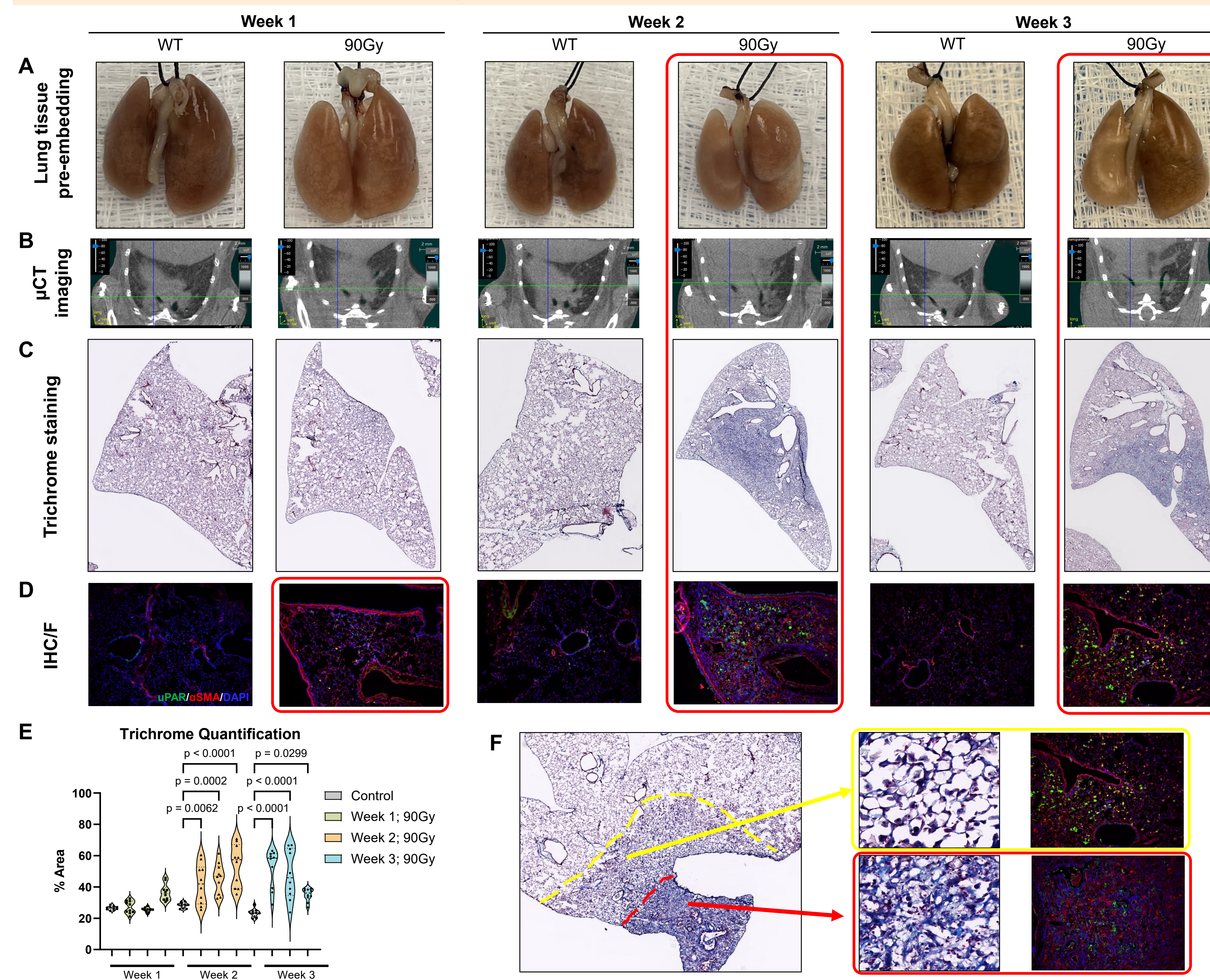


Figure 2. Development of a radiation induced pulmonary fibrosis (RIPF) mouse model. C57BL/6 mice were irradiated in the left lung with a single dose of 90 Gy, then monitored by multiple methods to observe development of RIPF (red frames). (A) Observation of lung tissue prior to sectioning shows tissue damage in the irradiated portion of the left lung, visible starting 2 weeks post-irradiation. (B) By CT imaging fibrosis is visible as opacity seen specifically in the left lungs of irradiated mice, beginning 2 weeks after irradiation. (C) Gomori Trichrome staining stains the collagen deposited in fibrotic regions blue, with dense blue regions visible in the left lungs of irradiated mice starting at 2 weeks post-irradiation. (D) Immunofluorescent staining reveals uPAR expression in the left lungs of irradiated animals, with uPAR expression seen as early as 1 week post-irradiation, an earlier phenotype than was observed with other methods. (E) Trichrome staining was quantified by determining the percent area stained blue of 10 random fields selected across the left lung. Significant increases in fibrosis measured by Trichrome staining were seen at 2 and 3 weeks after irradiation. (F) In lungs with visible fibrosis, regions of dense fibrosis (red) have fewer uPAR⁺ cells when compared to areas of developing or expanding fibrosis (yellow).

Primary murine CAR T cells specifically target and eliminate uPAR⁺ cells

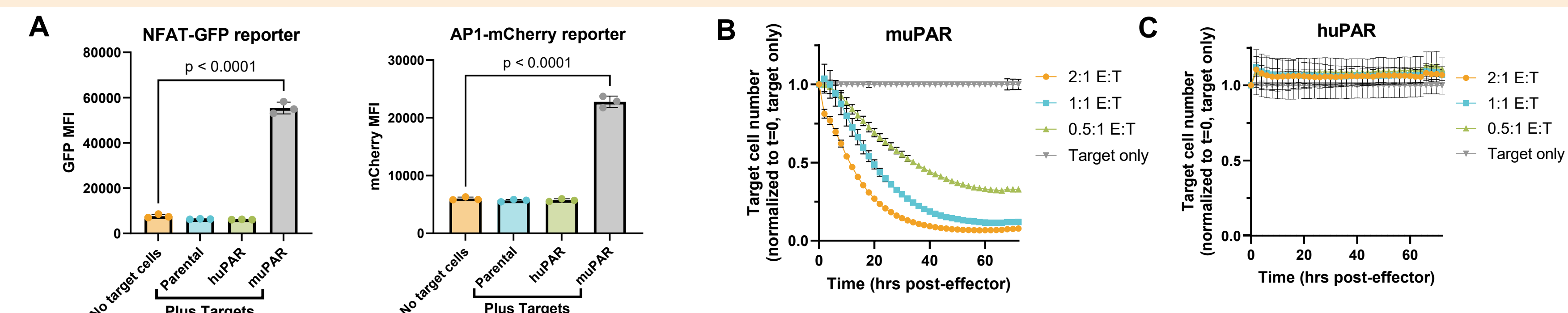


Figure 3. Generation and characterization of mouse primary uPAR CAR T cells. (A) A mouse uPAR CAR construct was transduced into Jurkat cells carrying fluorescent reporters for the NFAT (left) and AP1 (right) signaling pathways. The CAR transduced reporter cells induced signaling through T cell pathways in specific response to mouse, but not human, uPAR. The mouse uPAR CAR was then transduced into primary mouse T cells, which were used with Nalm6 target cells expressing mouse or human uPAR for in vitro Incucyte based assays. Mouse uPAR CAR T cells effectively kill target cells expressing mouse uPAR (B) with no observable response to human uPAR or other nonspecific activity (C).

Selection of human uPAR CAR binders based on domain specificity and affinity for pathologic levels of uPAR expression

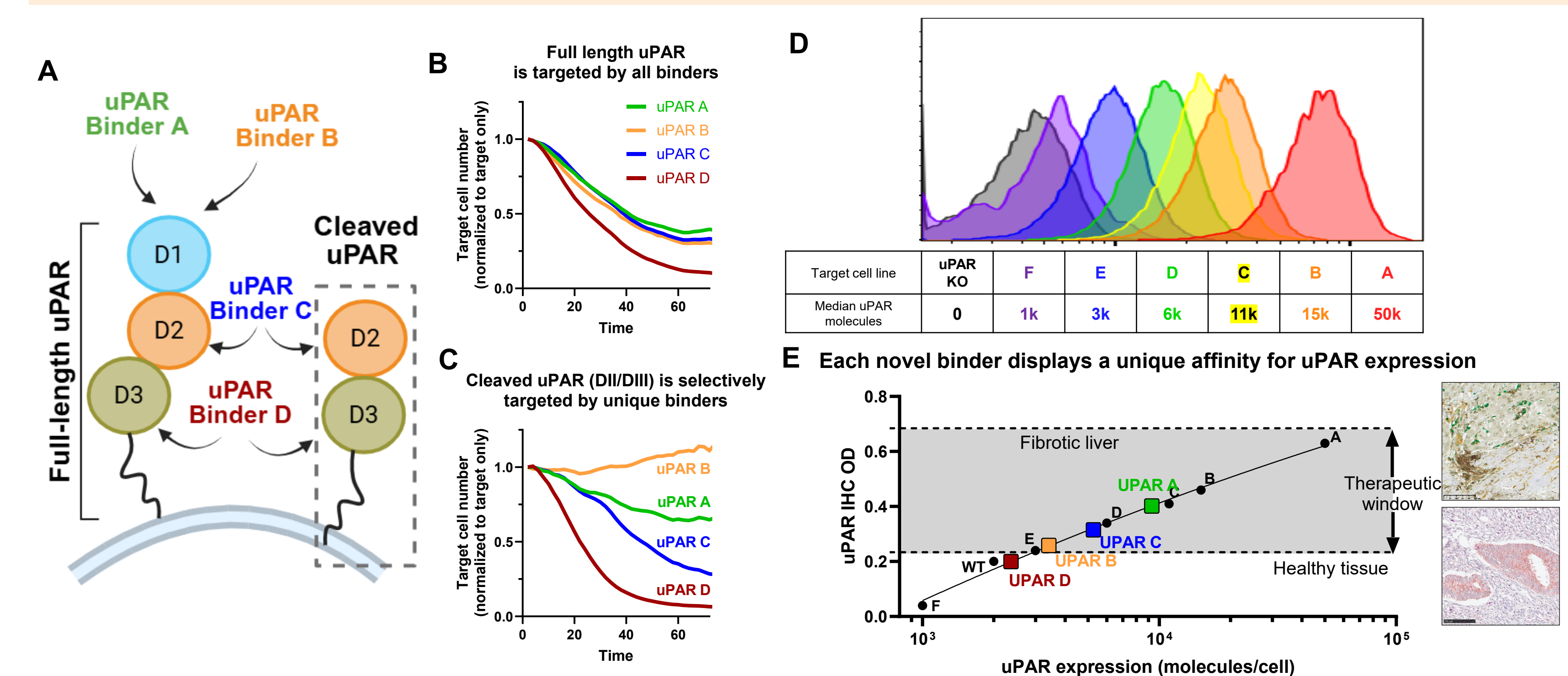


Figure 4. Characterization and ranking of human uPAR binders. Four different CAR binders targeting uPAR were transduced into primary human T cells and used to target Nalm6 cells overexpressing full length (B) or cleaved (C) uPAR. While all four uPAR CAR T cells could eliminate targets expressing full length uPAR, only uPAR C and uPAR D were effective against targets expressing cleaved uPAR. (A) uPAR protein is comprised of three extracellular domains and is frequently cleaved between domains 1 and 2. This schematic shows the approximate binding location of each uPAR CAR binder tested and their ability to target full length vs. cleaved uPAR. (D) A series of Nalm6 target lines were generated based on total uPAR expression, from low uPAR expression correlating with normal tissue (target line F) to higher uPAR levels as seen in MASH patient liver samples (target lines A-E). (E) By correlating uPAR expression on in vitro target lines with quantification of uPAR IHC in normal and disease patient samples we can arrange candidate uPAR binders by predicted activity against normal vs. pathologic tissue.

uPAR is expressed on a range of tumor cell lines, and human primary uPAR CAR T cells are effective in both in vitro and in vivo tumor models

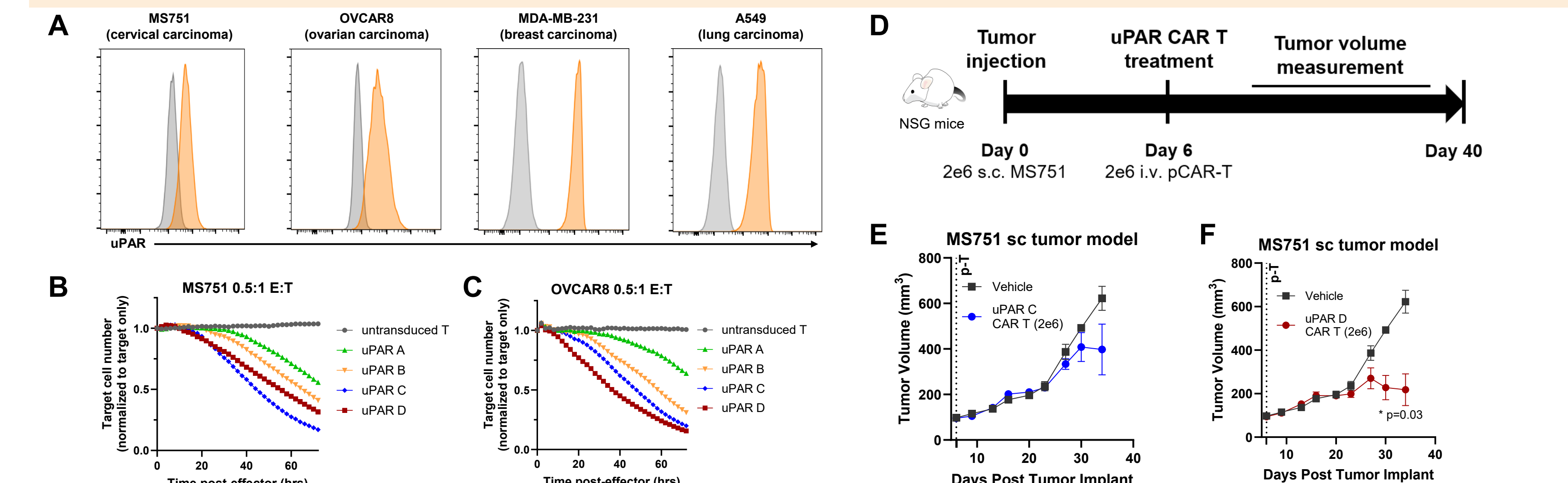


Figure 5. Anti-tumor activity of uPAR primary human CAR T cells. (A) Flow cytometry profiling of multiple model cell lines shows high surface expression of uPAR across multiple tumor models. Transduction of primary human T cells with lentiviruses encoding a series of uPAR CARs (Figure 4) enables the primary CAR T cells to kill MS751 (B) and OVCAR8 (C) target cells in an in vitro Incucyte assay. When injected intravenously into NSG mice with a MS751 based subcutaneous tumor (D), primary CAR T cells with the uPAR C (E) and uPAR D (F) binders both were able to control the volume of the tumor (graphs display mean SEM tumor volume, n=3 mice per group). uPAR D primary CAR T cells were more effective at controlling tumor growth than uPAR C CAR T cells, aligning with data showing a higher uPAR binding affinity in vitro (Figure 4E).

Targeting uPAR with multiplexed-engineered off-the-shelf CAR T cells enables unique strategies to eliminate fibrotic and oncogenic cells

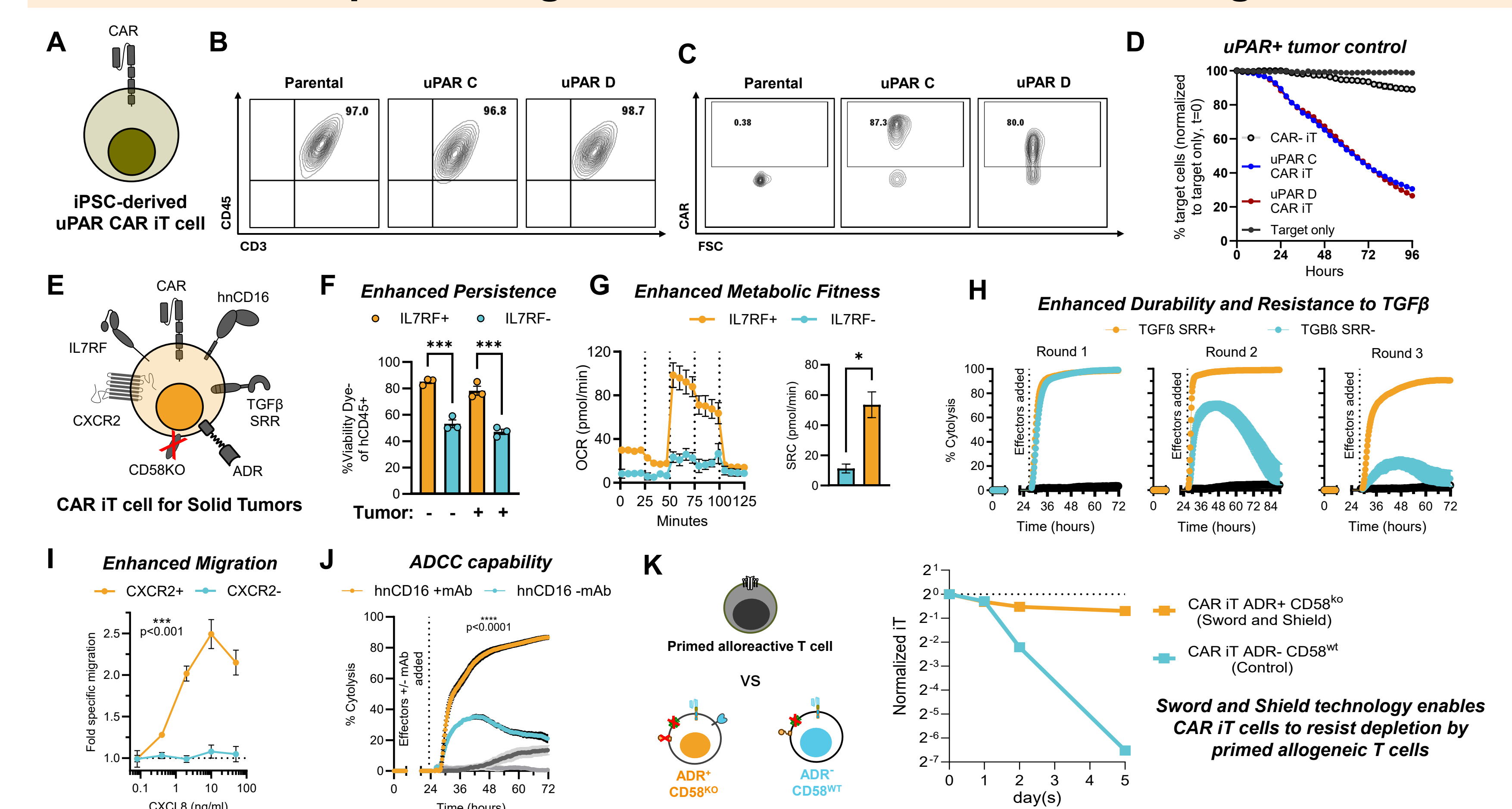


Figure 6. Demonstration of individual functional edits in Fate's off the shelf iPSC-derived CAR T cell platform. (A) Schematic illustrating minimally edited iPSC-derived CAR T cell targeting uPAR. (B) Transduction with two uPAR CAR lentiviruses does not alter the capacity to generate CD45⁺CD3⁺ iPSC-derived T cells. (C) After selection for CAR transduced cells, both uPAR CAR binders are highly expressed on iPSC-derived CAR T cells. (D) IT cells expressing uPAR CAR C or D (Figure 4) eliminate the uPAR expressing MS751 cervical carcinoma target cell line in an in vitro Incucyte-based assay. (E) Schematic illustrating the design of Fate's highly edited iPSC-derived CAR T cells. (F) IL7RF⁺ CAR IT cells have improved survival compared to IL7RF- CAR IT cells in the absence or presence of SKOV3 target cells in a flow cytometry-based viability assay. (G) IL7RF⁺ CAR IT cells exhibit increased oxygen consumption (OCR) and spare respiratory capacity (SRRC) when compared to IL7RF- CAR IT cells in a Seahorse metabolic assay. (H) TGF β SRRC CAR IT cells maintain anti-tumor activity against SKOV3 in the presence of TGF β over three rounds of a serial cytotoxicity assay, while TGF β SRRC- CAR IT cells rapidly lose cytotoxic activity after one round of co-culture with target cells. (I) CXCR2 CAR IT cells exhibit significantly higher CXCL8-dependent migration than CXCR2- CAR IT cells in an in vitro transwell assay. (J) hCD16⁺ CAR IT cells exhibit greater toxicity against SKOV3 target cells when combined with a therapeutic anti-EGFR monoclonal antibody. (K) CAR IT cells with Sword (ADR⁺) and Shield (CD58^{hi}) edits persist better in a co-culture with primed allogeneic T cells than CAR IT cells with no Sword and Shield edits.